UCLA
UCLA Previously Published Works

Title

Osteogenesis on nanoparticulate mineralized collagen scaffolds via autogenous activation of the canonical BMP receptor signaling pathway

Permalink

https://escholarship.org/uc/item/2bs2p26d

Journal

Biomaterials, 50(1)

ISSN

0267-6605

Authors

Ren, Xiaoyan
Bischoff, David
Weisgerber, Daniel W
et al.

Publication Date

2015-05-01

DOI

10.1016/j.biomaterials.2015.01.059

Peer reviewed

eScholarship.org Powered by the California Digital Library
University of California

Author Manuscript

Author Manuscript

Author Manuscript

Author Manuscript

HHS Public Access

Author manuscript

Biomaterials. Author manuscript; available in PMC 2015 November 01.

Published in final edited form as:

Biomaterials. 2015 May ; 50: 107–114. doi:10.1016/j.biomaterials.2015.01.059.

Osteogenesis on nanoparticulate mineralized collagen scaffolds via autogenous activation of the canonical BMP receptor signaling pathway

Xiaoyan Ren[a,b], **David Bischoff**[c], **Daniel W. Weisgerber**[d], **Michael S. Lewis**[e], **Victor Tu**[a,b], **Dean T. Yamaguchi**[c], **Timothy A. Miller**[a,b], **Brendan A.C. Harley**[d], and **Justine C. Lee**[a,b,*]

[a]Division of Plastic and Reconstructive Surgery, UCLA David Geffen School of Medicine, Los Angeles, CA 90095, USA

[b]Division of Plastic and Reconstructive Surgery, Greater Los Angeles VA Healthcare System, Los Angeles, CA 90073, USA

[c]Research Service, Greater Los Angeles VA Healthcare System, USA

[d]Department of Chemical and Biomolecular Engineering, Institute for Genomic Biology, University of Illinois at Urbana-Champaign, Urbana, IL 61801, USA

[e]Department of Pathology, Greater Los Angeles VA Healthcare System, USA

Abstract

Skeletal regenerative medicine frequently incorporates deliverable growth factors to stimulate osteogenesis. However, the cost and side effects secondary to supraphysiologic dosages of growth factors warrant investigation of alternative methods of stimulating osteogenesis for clinical utilization. In this work, we describe growth factor independent osteogenic induction of human mesenchymal stem cells (hMSCs) on a novel nanoparticulate mineralized collagen glycosaminoglycan scaffold (MC-GAG). hMSCs demonstrated elevated osteogenic gene expression and mineralization on MC-GAG with minimal to no effect upon addition of BMP-2 when compared to non-mineralized scaffolds (Col-GAG). To investigate the intracellular pathways responsible for the increase in osteogenesis, we examined the canonical and non-canonical pathways downstream from BMP receptor activation. Constitutive Smad1/5 phosphorylation with nuclear translocation occurred on MC-GAG independent of BMP-2, whereas Smad1/5 phosphorylation depended on BMP-2 stimulation on Col-GAG. When non-canonical BMPR signaling molecules were examined, ERK1/2 phosphorylation was found to be decreased in MC-GAG but elevated in Col-GAG. No differences in Smad2/3 or p38 activation were detected. Collectively, these results demonstrated that MC-GAG scaffolds induce osteogenesis without exogenous BMP-2 addition via endogenous activation of the canonical BMP receptor signaling pathway.

[*]Corresponding author: Division of Plastic and Reconstructive Surgery, UCLA David Geffen School of Medicine, 200 UCLA Medical Plaza, Suite 465, Los Angeles, CA 90095-6960, USA. Tel.:+1 310 794 7616; fax:+1 310 206 6833. justine@ucla.edu (J.C. Lee).

Author Manuscript Author Manuscript Author Manuscript Author Manuscript

Keywords

Osteogenesis; Biomimetic material; Nanoparticulate mineralization; BMP

1. Introduction

Skeletal regenerative medicine emerged as a field of investigation to address the current limitations for treating large osseous defects secondary to congenital, traumatic, and post-oncologic conditions. Although there is little debate that the optimal method of bone replacement is using completely autologous vascularized or non-vascularized bone, significant donor site morbidity occurs from harvesting bone [1–3].

Current methods for bone tissue engineering incorporate three elements: cells capable of undergoing osteogenic differentiation, growth factors, and scaffolding material [4,5]. The cellular component is frequently utilized to both initiate osteogenesis on the scaffold as well as to induce migration of osteogenic and angiogenic cells of the host environment. Growth factors are added to stimulate osteogenesis and potentially induce host site cells to differentiate into osteogenic cells. One of the most common family of growth factors used to induce osteogenesis is the bone morphogenetic protein (BMP) family [6]. To date, over 15 molecules of the BMP and growth and differentiation factor (GDF) subfamily have been identified and two have been approved for use in clinical medicine [7]. However, both cost and complications such ectopic bone formation, resorption, and decreased maxillary growth suggest that alternative clinical methods of inducing bone regeneration are warranted [8–10].

BMPs are first synthesized as precursor proteins that dimerize intracellularly. Upon dimerization, precursor proteins are cleaved at the consensus Arg-x-x-Arg site, yielding carboxy-terminal mature dimers that are secreted. Following secretion from cells, BMP dimers activate intracellular processes by binding to BMP receptor (BMPR) complexes [11]. Depending on the method of BMPR oligomerization, activation of the canonical or non-canonical pathways may occur (Fig. 1). In the canonical BMPR pathway, the receptor Smads (Smad1/5/8) are recruited and phosphorylated. Phosphorylated receptor Smads associate with co-Smad (Smad4) and translocate to the nucleus to activate transcription of various genes. In the non-canonical pathway, activation of ERK and p38 MAPK pathways occur. Both ERK and p38 MAPK have the capabilities to target receptor Smads for proteasomal degradation [12]. In addition, BMP receptors can also activate the Smad2/3 pathway as an additional non-canonical pathway. Although Smad2/3 is traditionally thought to be downstream of TGF-β receptor signaling, activation of the Smad2/3 pathway via BMP receptors has been reported in development and cancer [13,14].

Differences in scaffolding material have differential osteogenic properties depending on the material, porosity, and ability to mimic the organic and inorganic components of the normal extracellular matrix of bone [4]. Without the organic component, inorganic scaffolds based on calcium phosphate or calcium sulfate are osteoconductive but can be limited by variable resorption rates or brittle mechanical properties [15]. Without the inorganic component, collagen scaffolds lack structural strength and demonstrate significant contraction during

Author Manuscript Author Manuscript Author Manuscript Author Manuscript

mineralization [16–19]. The combination of collagen and mineral content has been evaluated previously and found to have promise in osteoconduction and bone healing, although the mechanism remains unknown and the superiority of such scaffolds in comparison to other types of scaffolds are unclear [20–23]. We have found that combining both the organic and inorganic components of the ECM in the form of a novel nanoparticulate mineralized collagen glycosaminoglycan (MC-GAG) scaffold results in a highly osteogenic and structurally stable scaffold for both primary rabbit bone marrow stromal cells and primary human mesenchymal stem cells [18,19,24,25]. In this work, we investigate osteogenic differentiation of human mesenchymal stem cells on MC-GAG scaffolds in conjunction with BMP-2 stimulation.

2. Materials and methods

2.1. Fabrication of non-mineralized and mineralized collagen scaffolds

Collagen-GAG scaffolds were prepared using the lyophilization process described previously [18,25,26]. Briefly, a suspension of collagen and GAGs or collagen-glycosaminoglycan-calcium phosphate (CGCaP) were produced by combining microfibrillar, type I collagen (Collagen Matrix, Oakland, NJ) and chondroitin-6-sulfate (Sigma–Aldrich, St. Louis, MO) in a solution of 0.05 M acetic acid (pH 3.2) or with calcium salts (calcium nitrate hydrate: $Ca(NO_3)_2{\cdot}4H_2O$; calcium hydroxide: $Ca(OH)_2$, Sigma–Aldrich) in a solution of phosphoric acid, respectively. The suspension was frozen using a constant cooling rate technique (1 °C/min) from room temperature to a final freezing temperature of −10 °C using a freeze dryer (Genesis, VirTis). The ice phase was sublimated under vacuum (<200 mTorr, 0 °C). Disks 5.8 mm in height and 8 mm in diameter were prepared using punch biopsies for cultures. Scaffold porosity was 85 ± 3% [27], pore size was 156 ± 6 μm [26,27], and morphology consisted of isotropic pores with a transverse:longitudinal pore aspect ratio of 0.95 ± 0.01 [26] as we previously reported. All scaffolds were sterilized via ethylene oxide.

2.2. Chemical crosslinking of mineralized and non-mineralized collagen scaffolds

Non-mineralized scaffolds (Col-GAG) and mineralized scaffolds (MC-GAG) were weighed before chemical crosslinking. These were placed into 100% ethanol under a laminar flow hood and left overnight. The scaffolds were then placed in serial dilutions of ethanol and phosphate buffered saline (PBS, Sigma Aldrich) every 2 h, to a final solution of 100% PBS, then allowed to hydrate overnight. Scaffolds were crosslinked in a solution of 1-ethyl-3-(3-dimethylaminopropyl) carbodiimide (EDC, Sigma Aldrich) and N-hydroxysuccinimide (NHS, Sigma Aldrich) at a molar ratio of 5:2:1 EDC:NHS:COOH where COOH represents the amount of collagen in the scaffold in distilled, deionized water for 2 h at room temperature [28]. The concentrations of EDC and NHS employed for crosslinking the scaffolds were based on previously established methods [26,29,30]. The concentration of EDC and NHS were based off of the dry weight of collagen within each scaffold. For mineralized scaffolds 0.0111 g/scaffold EDC and 0.0026 g/scaffold NHS were used. For non-mineralized control scaffolds, 0.0029 g/scaffold EDC and 0.0007 g/scaffold NHS were used. Both resulted in an identical crosslinking density [28]. After crosslinking, the scaffolds were washed in fresh PBS for an additional 2 h to remove any remaining chemical.

Author Manuscript Author Manuscript Author Manuscript Author Manuscript

2.3. Cell culture

hMSCs (Lonza, Inc., Allendale, NJ) were expanded in Corning cellgro Dulbecco's Modification of Eagle's (Mod.) (DMEM) supplemented with 10% fetal bovine serum (FBS) (Atlanta Biologicals, Atlanta, GA), 2 mM L-glutamine (Life Technologies, Carlsbad, CA), 100 IU/mL penicillin/100 μg/mL streptomycin (Life Technologies). At passage 3, 2×10^5 hMSCs were seeded onto 8-mm Col-GAG and MC-GAG scaffolds in proliferation media. 24 h after seeding, proliferation media was exchanged for osteogenic differentiation media consisting of 10 mM β-glycerophosphate, 50 μg/mL ascorbic acid and 0.1 μM dexamethasone. Scaffolds were untreated or treated with rhBMP-2 at a concentration of 50 ng/mL. Fresh BMP-2 (50 ng/mL) was added to each media change every 3 days.

2.4. Quantitative real-time reverse-transcriptase polymerase chain reaction

Scaffolds were processed for total RNA extraction using the RNeasy kit (Qiagen, Valencia, CA) at 0, 3, and 14 days. Gene sequences for β-actin, alkaline phosphatase (ALP), type I collagen (Col I), and osteopontin (OPN) were obtained from the National Center for Biotechnology Information gene database and oligonucleotide primers designed (Table 1). Quantitative real-time reverse-transcriptase polymerase chain reaction (RT-PCR) was performed on the Opticon Continuous Fluorescence System (Bio-Rad Laboratories, Inc., Hercules, CA) using the QuantiTect SYBR Green RT-PCR kit (Qiagen). Cycle conditions were as follows: reverse transcription at 50 °C (30 min); activation of HotStarTaq DNA polymerase/inactivation of reverse transcriptase at 95 °C (15 min); and 45 cycles of 94 °C for 15 s, 58 °C for 30 s, and 72 °C for 45 s. Results were analyzed using the comparative CT method for analyzing reverse-transcriptase polymerase chain reaction data and presented as representative graphs of triplicate experiments.

2.5. Western blot

Lysates for western blot analysis were prepared from scaffolds at 0, 3, 14, and 24 days of culture using Phosphosafe lysis buffer (Novagen, Madison, WI). Equal amounts of protein lysates were subjected to 4–20% SDS-PAGE (Bio-Rad, Hercules, CA). Western analysis was carried out with antibodies against phosphorylated Smad1/5 (p-Smad1/5), total Smad1/5/8, phosphorylated ERK1/2 (p-ERK1/2), total ERK1/2, phosphorylated Smad2/3 (p-Smad2/3), total Smad2/3, phosphorylated p38 (p-p38), total p38, and β-actin followed by 1:4000 dilutions of horseradish peroxidase-conjugated IgG antibodies (Bio-Rad, Hercules, CA) and an enhanced chemiluminescent substrate (Thermo Scientific, Rockford, IL). For detection of p-Smad1/5 and total Smad1/5/8, 40 μg of lysate was loaded per lane. For detection of p-ERK1/2 and total ERK1/2, 60 μg of lysate was loaded per lane. For detection p-p38, total p38, p-Smad2/3, total Smad2/3, 50 μg of lysate was loaded per lane. All primary phospho antibodies were obtained from Cell Signaling Technologies (Beverly, MA) and all primary full length antibodies were obtained from Santa Cruz Biotechnology (Santa Cruz, CA). Imaging was carried out using ImageJ (NIH, Bethesda, MD).

2.6. Histology and immunohistochemistry

Histologic studies were performed on scaffold cultures at 24 days and 6 weeks. Scaffolds were fixed at 10% normal buffered formalin, embedded in paraffin, and sectioned at 4

Author Manuscript Author Manuscript Author Manuscript Author Manuscript

microns using standard techniques. The sections were deparaffinized and stained with hematoxylin and eosin, Alizarin Red, or anti-p-Smad1/5 (Cell Signaling Technologies, Beverly, MA) and processed with the Dako automated FLEX system (Dako, Carpinteria, CA). All slides were analyzed qualitatively using a standard microscope and digitally photographed at 20× magnification.

2.7. Micro–computed tomographic imaging

Mineralization was followed by micro–computed tomographic imaging (μCT) using the Scanco μCT 35 (Scanco Medical AG, Bruttisellen, Switzerland) at 6 and 12 weeks in culture (n = 3 scaffolds per timepoint). Scaffolds were fixed using 10% formalin for 24 h and stored in 70% ethanol at 4 °C. Scans were performed using medium resolution settings with a source voltage of 70 E (kVp) and I (μA) of 114. The images had a final element size of 12.5 μm. Two-dimensional images were analyzed using software supplied from Scanco (Image Processing Language version 5.6). Scaffold areas were contoured to establish volumes of interest by visual examination of serial slices in all of the specimens. Optimum arbitrary threshold values of 20 (showing scaffold and mineralization) and 80 (mineralization alone) were used uniformly for all specimens to quantify mineralized areas from surrounding unmineralized scaffold.

Histomorphometric analysis of three-dimensional reconstructions was performed using Scanco Evaluation scripts no. 2 (three-dimensional segmentation of two volumes of interest: solid dense in transparent low-density object) for three-dimensional images and script no. 6 (bone volume/density only bone evaluation) for volume determinations.

2.8. Statistical analysis

Computer-assisted statistical analyses were performed using SigmaStat 3.5 (Systat Software, Inc., San Jose, CA). Data points were composed of duplicates of at least three independent experiments, unless otherwise indicated. Mean measurements of mRNA expression were analyzed for statistical significance by either analysis of variance or independent Student's t-test, as appropriate. A value of $p < 0.05$ was considered significant.

3. Results

3.1. Mineralized collagen glycosaminoglycan scaffolds upregulate alkaline phosphatase, osteopontin, and collagen I expression in bone marrow derived human mesenchymal stem cells

hMSCs ($CD105^+CD166^+CD29^+CD44^+CD14^-CD34^-CD45^-$) from a bone marrow source were cultured in osteogenic differentiation medium on Col-GAG or MC-GAG scaffolds treated with and without BMP-2. Total RNA isolated at 0, 3, and 14 days in culture were subjected to quantitative RT-PCR in triplicate (Fig. 2). All genes were reported as a relative change in expression levels in relationship to day 0 expression. On day 3, expression of alkaline phosphatase (ALP) was somewhat increased in BMP-2 treated MC-GAG scaffolds in comparison to BMP-2 treated Col-GAG scaffolds. No statistically significant differences were noted in treated versus untreated scaffolds for either Col-GAG or MC-GAG. By day 14, MC-GAG scaffolds expressed more ALP both with and without BMP-2 treatment in

Author Manuscript Author Manuscript Author Manuscript Author Manuscript

comparison to Col-GAG scaffolds in a statistically significant manner. Addition of BMP-2 to day 14 cultures on MC-GAG scaffolds added only a modest increase in ALP expression. For collagen I (Col I), minimal to no differences in gene expression occurred on day 3. On day 14, only the MC-GAG scaffolds demonstrated an elevation of Col I transcripts both in the absence and presence of BMP-2. Addition of BMP-2 did not result in a statistically significant increase in Col I expression in MC-GAG scaffolds. Lastly, osteopontin (OPN) expression displayed increases in both day 3 and 14 of culture in the MC-GAG scaffolds in comparison to Col-GAG scaffolds with and without BMP-2 stimulation. Again, BMP-2 did not have a statistically significant effect on OPN gene expression.

For both timepoints, all three genes showed statistically significant increases in osteogenic gene expression for the MC-GAG scaffolds in comparison to the Col-GAG scaffolds. Interestingly, exogenous BMP-2 stimulation had only a minor effect on osteogenic gene expression suggesting that addition of mineral content is more osteogenic than exogenous BMP-2 stimulation.

3.2. Mineralization of hMSCs is increased in response to nanoparticulate mineralized collagen-GAG scaffolds

To investigate whether the increases in osteogenic gene expression translated to increased mineralization, hMSCs-seeded on Col-GAG and MC-GAG scaffolds in the presence and absence of BMP-2 (50 ng/mL) were subjected to histologic analysis (Fig. 3) and μCT scanning (Fig. 4).

Similar to the gene expression studies, mineralization of hMSCs was more robust in the MC-GAG scaffolds in comparison to the Col-GAG scaffolds at both day 24 and 6 weeks of culture in Alizarin Red staining (Fig. 3). Again, BMP-2 had, at best, a modest effect for hMSCs at day 24 on Col-GAG scaffolds but no obvious increases in mineralization for MC-GAG scaffolds. Of note, all of the mineralized content in Col-GAG scaffolds at the 6 week timepoint was found at the surfaces of the scaffold.

At 6 and 12 weeks of culture, μCT scanning confirmed that mineralization was significantly increased in MC-GAG scaffolds in comparison to Col-GAG scaffolds (Fig. 4). While MC-GAG scaffolds showed mineralized content throughout the entirety of the scaffold, mineralization was limited to the surface of Col-GAG scaffolds at either timepoint. An analysis of the percent mineralized volume to total scaffold in triplicate (Fig. 4B) showed statistically significant differences in MC-GAG versus Col-GAG scaffolds whereas no differences were found in the presence or absence of BMP-2. Although a small amount of mineralization occurred in either scaffold when incubated in cell free medium for 6 and 12 weeks, the amount of mineralization was minimal in comparison to the mineralization achieved with cellular content. This confirms that addition of mineral content to Col-GAG scaffolds surpasses the effects of BMP-2 stimulation on osteogenesis and mineralization of hMSCs.

Author Manuscript Author Manuscript Author Manuscript Author Manuscript

3.3. Constitutive Smad1/5 phosphorylation in hMSCs on MC-GAG scaffolds with decreased ERK phosphorylation

To elucidate the mechanism behind increased osteogenesis in MC-GAG scaffolds in relationship to Col-GAG scaffolds, the Smad dependent and independent pathways of BMP receptor signaling were investigated (Fig. 5). In Col-GAG scaffolds, phosphorylated Smad1/5 (p-Smad1/5) was demonstrated in response to BMP-2 stimulation at all three timepoints. Minimal amounts of p-Smad1/5 were detected in the untreated Col-GAG scaffolds. Total Smad1/5 and actin western blots showed equal total Smad1/5 expression across all of the scaffolds. MC-GAG scaffolds were dramatically different in both the quantity of Smad1/5 phosphorylation and response to BMP-2. Even at day 0, MC-GAG scaffolds showed significant p-Smad1/5. P-Smad1/5 was slightly increased at days 14 and 24 in BMP-2 treated scaffolds but was also strongly detected in untreated scaffolds. Again, total Smad1/5 and actin demonstrated equal protein expression in all scaffolds. These data demonstrated that the BMPR canonical pathway is constitutively activated in MC-GAG scaffolds with minimal additional activation in the presence of exogenous BMP-2.

To evaluate the non-canonical BMP receptor pathways for comparison to Smad1/5 activation, phosphorylated ERK1/2 (p-ERK1/2), phosphorylated p38 (p-p38), and phosphorylated Smad2/3 (p-Smad2/3) were compared to the respective total protein (Fig. 5B–D). In contrast to Smad phosphorylation, p-ERK1/2 was elevated in the Col-GAG scaffolds in comparison to the MC-GAG scaffolds. At day 0, p-ERK1/2 was found in abundance in Col-GAG scaffolds whereas a comparatively small amount of p-ERK1/2 was detected in MC-GAG scaffolds. At both days 14 and 24, BMP-2 stimulation resulted in a slight reduction in p-ERK1/2 in Col-GAG and MC-GAG scaffolds. Both total ERK1/2 and actin expression were equal in all of the scaffolds. No differences in p-p38, p-Smad2/3, or their respective total proteins were detected (Fig. 4C and D). These data show that MC-GAG scaffolds downregulate ERK1/2 phosphorylation. Interestingly, BMP-2 stimulation downregulates ERK1/2 expression at later timepoints in either non-mineralized or mineralized scaffolds.

3.4. Phosphorylated Smad1/5 translocates to the nucleus in both Col-GAG and MC-GAG scaffolds

Following phosphorylation, Smad1/5 translocates to the nucleus to activate transcription of downstream targets. To confirm that the p-Smad1/5 detected in western blots was capable of nuclear translocation, Col-GAG and MC-GAG scaffolds seeded with hMSCs at 24 days and 6 weeks of culture, untreated and treated with BMP-2 stimulation, were subjected to immunohistochemistry with an antibody against p-Smad1/5 (Fig. 6). Strong staining and nuclear localization of p-Smad1/5 was seen in the presence and absence of BMP-2 in MC-GAG scaffolds at both timepoints. Col-GAG also demonstrated nuclear p-Smad1/5 staining at day 24. Similar to the Alizarin red staining (Fig. 3) and micro-CT data (Fig. 4A), the p-Smad1/5 staining could only detected at the most peripheral edges of the scaffold. At 6 weeks of culture, p-Smad1/5 was no longer detected on Col-GAG scaffolds even at the most peripheral aspects of the scaffold.

Author Manuscript Author Manuscript Author Manuscript Author Manuscript

4. Discussion

In this work, we investigated the contribution of exogenous BMP-2 stimulation to osteogenic differentiation of hMSCs on mineralized collagen glycosaminoglycan scaffolds. Interestingly, our data showed that MC-GAG scaffolds were independently efficient at osteogenic gene expression and mineralization of hMSCs. The addition of BMP-2 resulted in a modest increase of alkaline phosphatase expression and no statistically significant differences in expression of other osteogenic genes or mineralization. To elucidate the signaling molecules that may contribute to this effect, we demonstrated that the canonical BMP receptor Smads (Smad1/5) were constitutively phosphorylated in MC-GAG scaffolds with or without BMP-2 stimulation, whereas phosphorylated Smad1/5 was largely dependent on BMP-2 stimulation in Col-GAG scaffolds. On examination of three non-canonical BMP receptor signaling pathway molecules, ERK1/2 phosphorylation was the only factor that demonstrated differences between Col-GAG and MC-GAG scaffolds. With respect to Smad1/5 phosphorylation, ERK1/2 phosphorylation showed an inverse relationship to the two scaffolds. In Col-GAG scaffolds, greater amounts of p-ERK1/2 were found in comparison to MC-GAG, especially at the earliest time-points. At days 14 and 24, both Col-GAG and MC-GAG scaffolds showed decreased p-ERK1/2 in response to BMP-2 stimulation. For both p38 and Smad2/3, a baseline level of phosphorylated proteins was seen in both scaffolds at all timepoints. Lastly, p-Smad1/5 nuclear translocation was clearly demonstrated in both Col-GAG and MC-GAG scaffolds. Unlike MC-GAG scaffolds where p-Smad1/5 positive cells were easily detected throughout the scaffold, Col-GAG scaffolds only showed p-Smad1/5 positive cells at the peripheral edges of the scaffold on day 24. By 6 weeks, no p-Smad1/5 could be detected in Col-GAG scaffolds while MC-GAG continued to show robust nuclear staining.

The combination of our current work raises several questions on scaffold biology and osteogenic differentiation of hMSCs. First, a common theme in the hMSC-mediated mineralization of scaffolds is that Col-GAG scaffolds reproducibly showed osteogenic differentiation and mineralization at the periphery whereas MC-GAG demonstrated excellent mineralization throughout the entirety of the scaffold. This phenomenon correlated to the distribution of hMSCs on the scaffold. While there are only slight differences in porosity of the scaffolds, previous studies showed that Col-GAG and MC-GAG scaffolds differed in terms of both the presence of nanoparticulate calcium phosphate particles as well as increased elastic moduli [25,26]. Several investigators have proposed a role for inorganic ions in stimulating osteogenic differentiation of various progenitor cell types and cell lines [31–34]. Specifically, phosphate ion has generated excitement in the field of vascular biology due to an increased propensity for intravascular calcification with hyperphosphatemia seen in chronic renal disease [35,36]. The mechanism behind phosphate-induced osteogenesis has been partially elucidated to involve the ubiquitous sodium phosphate cotransporter SLC20a1, adenosine signaling, and ERK1/2 phosphorylation [34,37,38]. Because ERK1/2 phosphorylation was seen in lower amounts in MC-GAG scaffolds, it is likely that calcium phosphate may contribute to osteogenic differentiation and cell migration in a slightly different manner than the reported mechanism. One possibility is that the mineral content stimulates BMP receptor oligomerization thereby constitutively

Author Manuscript Author Manuscript Author Manuscript Author Manuscript

activating the BMP receptor signaling pathway. Another possibility is that intracellular transport of calcium or phosphate ions inhibits negative regulators of the Smad signaling pathway such as Smad6 or Smad7. The separate contributions of calcium versus phosphate in osteogenic differentiation may be an interesting avenue for future studies.

MC-GAG scaffolds demonstrated a decreased amount of ERK1/2 phosphorylation in comparison to Col-GAG scaffolds. In both Col-GAG and MC-GAG scaffolds, BMP-2 stimulation actually decreased the amount of ERK1/2 phosphorylation detected on western blots. Similar to hMSCs, we have recently shown that ERK1/2 downregulation occurs in primary rabbit bone marrow stromal cells undergoing osteogenic differentiation [39]. Our laboratory has also previously reported that ERK1/2 activation inhibits osteogenic differentiation of MC3T3-E1 cells in three-dimensional systems [40]. In combination, our current data and previous work suggest that the canonical BMPR signaling pathway is preferentially induced during osteogenic differentiation in three-dimensional cultures across multiple progenitor cell types and across species.

5. Conclusions

Clinically, the limited availability of autologous bone for skeletal replacement has resulted in the development of various alloplastic implants and usage of recombinant growth factors. For complicated wounds such as radiated tissues or composite tissue deficiencies, alloplastic implant failures range from 16 to 62% from extrusion or infection [3,41–43]. Outcomes studies of BMP-2 usage are now showing evidence of complications such as heterotopic ossification, resorption, disturbances in maxillary growth, and elevated cancer rates [10,44]. It is clear that neither of the former methods are adequate universal solutions for clinical use. Methods that minimize or eliminate the reliance on artificial implants and growth factors are essential areas for investigation. In this work, our finding that a novel mineralized collagen glycosaminoglycan scaffold independently induced robust osteogenesis without BMP-2 stimulation lays the groundwork on a host of clinical possibilities based on biomaterials and cellular infiltration without the untoward effects of supraphysiologic growth factor stimulation.

Acknowledgments

This work was supported by a Merit Review Grant (1I01BX001367-01A2) awarded by the U.S. Department of Veterans Affairs (TAM) and the Jean Perkins Foundation (JCL). Research reported in this publication was also supported by the National Institute of Arthritis and Musculoskeletal and Skin Diseases of the National Institutes of Health under Award Numbers R21 AR063331 (BACH). The content is solely the responsibility of the authors and does not necessarily represent the official views of the National Institutes of Health. DWW was funded at UIUC from National Science Foundation (NSF) Grant 0965918 IGERT: Training the Next Generation of Researchers in Cellular & Molecular Mechanics and BioNanotechnology.

References

1. Ebraheim NA, Elgafy H, Xu R. Bone-graft harvesting from iliac and fibular donor sites: techniques and complications. J Am Acad Orthop Surg. 2001; 9:210–8. [PubMed: 11421578]
2. Arrington ED, Smith WJ, Chambers HG, Bucknell AL, Davino NA. Complications of iliac crest bone graft harvesting. Clin Orthop Relat Res. 1996:300–9. [PubMed: 8769465]

Author Manuscript Author Manuscript Author Manuscript Author Manuscript

3. Lee JC, Kleiber GM, Pelletier AT, Reid RR, Gottlieb LJ. Autologous immediate cranioplasty with vascularized bone in high-risk composite cranial defects. Plast Reconstr Surg. 2013; 132:967–75. [PubMed: 24076686]
4. Szpalski C, Wetterau M, Barr J, Warren SM. Bone tissue engineering: current strategies and techniques–part I: Scaffolds. Tissue Eng Part B Rev. 2012; 18:246–57. [PubMed: 22029448]
5. Szpalski C, Sagebin F, Barbaro M, Warren SM. The influence of environmental factors on bone tissue engineering. J Biomed Mater Res B Appl Biomater. 2013 May; 101(4):663–75. [PubMed: 23165885]
6. Ducy P, Karsenty G. The family of bone morphogenetic proteins. Kidney Int. 2000; 57:2207–14. [PubMed: 10844590]
7. Mueller TD, Nickel J. Promiscuity and specificity in BMP receptor activation. FEBS Lett. 2012; 586:1846–59. [PubMed: 22710174]
8. Lewandrowski KU, Nanson C, Calderon R. Vertebral osteolysis after posterior interbody lumbar fusion with recombinant human bone morphogenetic protein 2: a report of five cases. Spine J. 2007; 7:609–14. [PubMed: 17526434]
9. Smoljanovic T, Bojanic I, Delimar D. Adverse effects of posterior lumbar interbody fusion using rhBMP-2. Eur Spine J. 2009; 18:920–3. [author reply 4]. [PubMed: 19352727]
10. Yee KS, Nguyen PD, Andrews BT, Lee JC, Bradley JP. Abstract 4: decreased secondary bone grafting but poorer midface growth after primary alveolar cleft repair with gingivoperiosteoplasty and rhBMP-2. Plast Reconstr Surg. 2014; 133:975.
11. Miyazono K, Kamiya Y, Morikawa M. Bone morphogenetic protein receptors and signal transduction. J Biochem. 2010; 147:35–51. [PubMed: 19762341]
12. Kretzschmar M, Doody J, Massagué J. Opposing BMP and EGF signalling pathways converge on the TGF-beta family mediator Smad1. Nature. 1997; 389:618–22. [PubMed: 9335504]
13. Wang Y, Ho CC, Bang E, Rejon CA, Libasci V, Pertchenko P, et al. Bone morphogenetic protein 2 stimulates noncanonical SMAD2/3 signaling via the BMP type 1A receptor in gonadotrope-like cells: implications for FSH synthesis. Endocrinology. 2014; 155:1970–81. [PubMed: 24601881]
14. Holtzhausen A, Golzio C, How T, Lee YH, Schiemann WP, Katsanis N, et al. Novel bone morphogenetic protein signaling through Smad2 and Smad3 to regulate cancer progression and development. FASEB J. 2014; 28:1248–67. [PubMed: 24308972]
15. Walsh WR, Vizesi F, Michael D, Auld J, Langdown A, Oliver R, et al. Beta-TCP bone graft substitutes in a bilateral rabbit tibial defect model. Biomaterials. 2008; 29:266–71. [PubMed: 18029011]
16. Kruger EA, Im DD, Bischoff DS, Pereira CT, Huang W, Rudkin GH, et al. In vitro mineralization of human mesenchymal stem cells on three-dimensional type I collagen versus PLGA scaffolds: a comparative analysis. Plast Reconstr Surg. 2011; 127:2301–11. [PubMed: 21617464]
17. Zeng X, Zeng YS, Ma YH, Lu LY, Du BL, Zhang W, et al. Bone marrow mesenchymal stem cells in a three-dimensional gelatin sponge scaffold attenuate inflammation, promote angiogenesis, and reduce cavity formation in experimental spinal cord injury. Cell Transplant. 2011; 20:1881–99. [PubMed: 21396163]
18. Harley BA, Lynn AK, Wissner-Gross Z, Bonfield W, Yannas IV, Gibson LJ. Design of a multiphase osteochondral scaffold. II. Fabrication of a mineralized collagen-glycosaminoglycan scaffold. J Biomed Mater Res A. 2010; 92:1066–77. [PubMed: 19301274]
19. Lee JC, Pereira CT, Ren X, Huang W, Bischoff D, Weisgerber DW, et al. Optimizing collagen scaffolds for bone engineering: effects of crosslinking and mineral content on structural contraction and osteogenesis. J Craniofac Surg. 2014 [submitted].
20. Du C, Cui FZ, Zhu XD, de Groot K. Three-dimensional nano-HAp/collagen matrix loading with osteogenic cells in organ culture. J Biomed Mater Res. 1999; 44:407–15. [PubMed: 10397944]
21. Lickorish D, Ramshaw JA, Werkmeister JA, Glattauer V, Howlett CR. Collagen-hydroxyapatite composite prepared by biomimetic process. J Biomed Mater Res A. 2004; 68:19–27. [PubMed: 14661245]
22. Rodrigues CV, Serricella P, Linhares AB, Guerdes RM, Borojevic R, Rossi MA, et al. Characterization of a bovine collagen-hydroxyapatite composite scaffold for bone tissue engineering. Biomaterials. 2003; 24:4987–97. [PubMed: 14559012]

Author Manuscript Author Manuscript Author Manuscript Author Manuscript

23. Liao SS, Cui FZ, Zhang W, Feng QL. Hierarchically biomimetic bone scaffold materials: nano-HA/collagen/PLA composite. J Biomed Mater Res B Appl Biomater. 2004; 69:158–65. [PubMed: 15116405]
24. Weisgerber DW, Caliari SR, Harley BA. Selective addition of mineral into collagen scaffolds to enhance hMSC osteogenesis and matrix remodeling. Acta Biomater. 2014 in press.
25. Harley BA, Leung JH, Silva EC, Gibson LJ. Mechanical characterization of collagen-glycosaminoglycan scaffolds. Acta Biomater. 2007; 3:463–74. [PubMed: 17349829]
26. Weisgerber DW, Kelkhoff DO, Caliari SR, Harley BAC. The impact of discrete compartments of a multi-compartment collagen-GAG scaffold on overall construct biophysical properties. J Mech Behav Biomed Mater. 2013; 28:26–36. [PubMed: 23973610]
27. Harley BA, Lynn AK, Wissner-Gross Z, Bonfield W, Yannas IV, Gibson LJ. Design of a multiphase osteochondral scaffold II: fabrication of a mineralized collagen-GAG scaffold. J Biomed Mater Res A. 2010; 92:1066–77. [PubMed: 19301274]
28. Olde Damink LH, Dijkstra PJ, van Luyn MJ, van Wachem PB, Nieuwenhuis P, Feijen J. Cross-linking of dermal sheep collagen using a water-soluble carbodiimide. Biomaterials. 1996; 17:765–73. [PubMed: 8730960]
29. Caliari SR, Gonnerman EA, Grier WK, Weisgerber DW, Banks JM, Alsop AJ, et al. Collagen scaffold arrays for combinatorial screening of biophysical and biochemical regulators of cell behavior. Adv Healthc Mater. 2014
30. Caliari SR, Harley BAC. Structural and biochemical modification of a collagen scaffold to selectively enhance MSC tenogenic, chondrogenic, and osteogenic differentiation. Adv Healthc Mater. 2014; 3:1086–96. [PubMed: 24574180]
31. Tang Z, Wang Z, Qing F, Ni Y, Fan Y, Tan Y, et al. Bone morphogenetic protein Smads signaling in mesenchymal stem cells affected by osteoinductive calcium phosphate ceramics. J Biomed Mater Res A. 2015 Mar; 103(3):1001–10. [PubMed: 24889783]
32. Eyckmans J, Roberts SJ, Schrooten J, Luyten FP. A clinically relevant model of osteoinduction: a process requiring calcium phosphate and BMP/Wnt signalling. J Cell Mol Med. 2010; 14:1845–56. [PubMed: 19538476]
33. Cushnie EK, Ulery BD, Nelson SJ, Deng M, Sethuraman S, Doty SB, et al. Simple signaling molecules for inductive bone regenerative engineering. PLoS One. 2014; 9:e101627. [PubMed: 25019622]
34. Shih YR, Hwang Y, Phadke A, Kang H, Hwang NS, Caro EJ, et al. Calcium phosphate-bearing matrices induce osteogenic differentiation of stem cells through adenosine signaling. Proc Natl Acad Sci U S A. 2014; 111:990–5. [PubMed: 24395775]
35. Russo D, Bellasi A, Pota A, Russo L, Di Iorio B. Effects of phosphorus-restricted diet and phosphate-binding therapy on outcomes in patients with chronic kidney disease. J Nephrol. 2014 Mar 6. [Epub ahead of print].
36. Shroff R. Phosphate is a vascular toxin. Pediatr Nephrol. 2013; 28:583–93. [PubMed: 23161206]
37. Julien M, Khoshniat S, Lacreusette A, Gatius M, Bozec A, Wagner EF, et al. Phosphate-dependent regulation of MGP in osteoblasts: role of ERK1/2 and Fra-1. J Bone Miner Res. 2009; 24:1856–68. [PubMed: 19419315]
38. Khoshniat S, Bourgine A, Julien M, Petit M, Pilet P, Rouillon T, et al. Phosphate-dependent stimulation of MGP and OPN expression in osteoblasts via the ERK1/2 pathway is modulated by calcium. Bone. 2011; 48:894–902. [PubMed: 21147284]
39. Ren X, Bischoff D, Weisgerber DW, Tu V, Lewis MS, Yamaguchi DT, et al. Nanoparticulate mineral content in collagen scaffolds increases osteogenesis independent of exogenous BMP-2 in bone marrow stromal cells. 2014 [submitted].
40. Im DD, Kruger EA, Huang WR, Sayer G, Rudkin GH, Yamaguchi DT, et al. Extracellular-signal-related kinase 1/2 is responsible for inhibition of osteogenesis in three-dimensional cultured MC3T3-E1 cells. Tissue Eng Part A. 2010; 16:3485–94. [PubMed: 20590408]
41. Shonka DC, Potash AE, Jameson MJ, Funk GF. Successful reconstruction of scalp and skull defects: lessons learned from a large series. Laryngoscope. 2011; 121:2305–12. [PubMed: 22020883]

Author Manuscript Author Manuscript Author Manuscript Author Manuscript

42. Afifi A, Djohan RS, Hammert W, Papay FA, Barnett AE, Zins JE. Lessons learned reconstructing complex scalp defects using free flaps and a cranioplasty in one stage. J Craniofac Surg. 2010; 21:1205–9. [PubMed: 20613618]

43. Zins JE, Moreira-Gonzalez A, Papay FA. Use of calcium-based bone cements in the repair of large, full-thickness cranial defects: a caution. Plast Reconstr Surg. 2007; 120:1332–42. [PubMed: 17898609]

44. Tannoury CA, An HS. Complications with the use of bone morphogenetic protein 2 (BMP-2) in spine surgery. Spine J. 2014; 14:552–9. [PubMed: 24412416]

Author Manuscript Author Manuscript Author Manuscript Author Manuscript

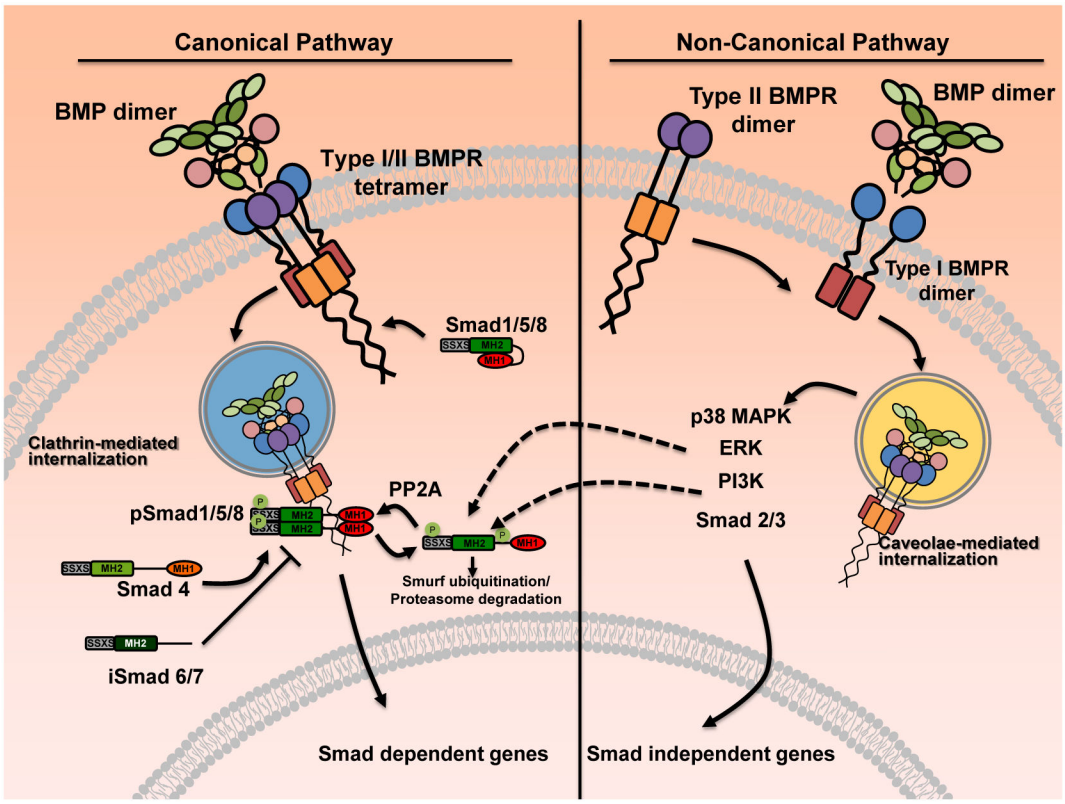

Fig. 1.

BMP receptor mediated pathways. The canonical BMP receptor mediated pathway is activated upon ligand binding with the BMPR tetramer composed of type I and type II dimers. Upon binding, the BMP receptor Smads (Smad1/5/8) are recruited to the receptor complex and phosphorylated. Phosphorylated Smad1/5/8 bind to Smad4 (the co-Smad) resulting in nuclear translocation and transactivation of osteogenic genes. In the non-canonical pathway, BMP binds to the type I BMPR dimer thereby recruiting type II BMPR dimers. The assembled receptor/ligand complex is then internalized and various intracellular signaling molecules are activated including the p38 MAPK, ERK1/2, PI3K/Akt, and the Smad2/3.

Author Manuscript Author Manuscript Author Manuscript Author Manuscript

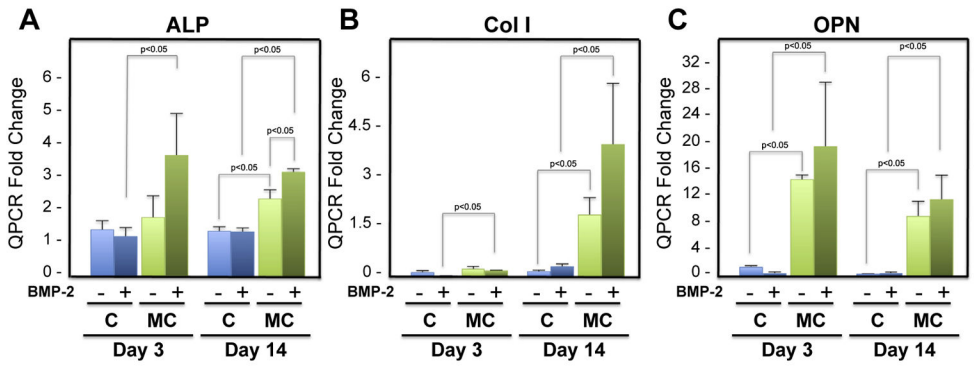

Fig. 2.

Relative mRNA expression of alkaline phosphatase, collagen I, and osteopontin in hMSCs in response to BMP-2 on Col-GAG and MC-GAG scaffolds. Real-time RT-PCR analysis of A) alkaline phosphatase (ALP), B) collagen I (Col I), and C) osteopontin (OPN) expression of hMSCs with and without BMP-2 (50 ng/mL) treatment in Col-GAG and MC-GAG scaffolds at days 3 and 14 of culture. Data is expressed as the mean ± SD of three independent experiments. P value is shown in the figure.

Author Manuscript Author Manuscript Author Manuscript Author Manuscript

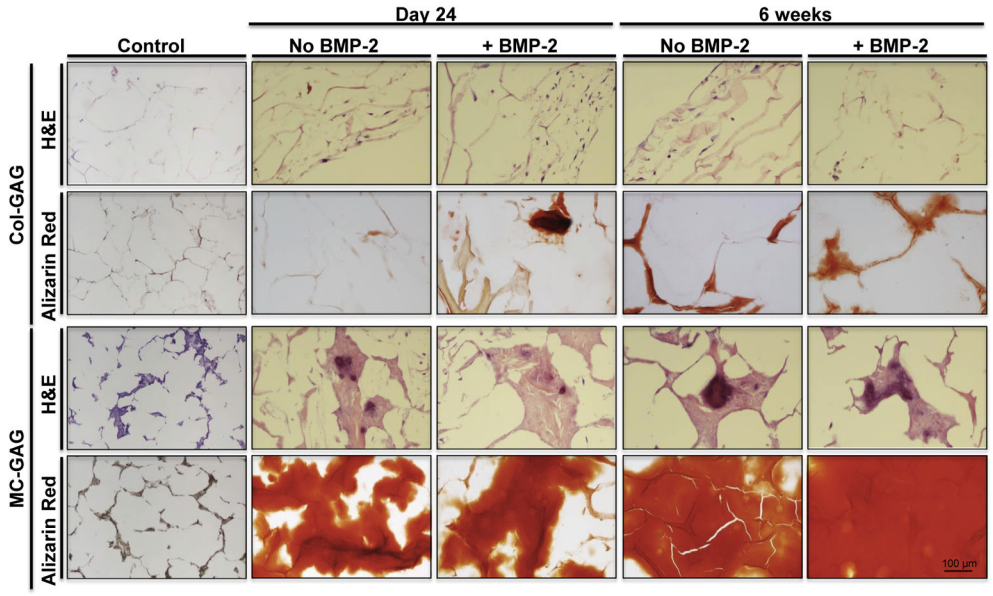

Fig. 3.

Histology of hMSCs undergoing osteogenesis on Col-GAG and MC-GAG scaffolds in the absence and presence of BMP-2. H&E and Alizarin Red staining of histologic sections of Col-GAG and MC-GAG scaffolds cultured with hMSCs in osteogenic medium in the presence or absence of BMP-2 (50 ng/mL) for 24 days or 6 weeks. (Magnification, 20×). (For interpretation of the references to color in this figure legend, the reader is referred to the web version of this article.)

Author Manuscript Author Manuscript Author Manuscript Author Manuscript

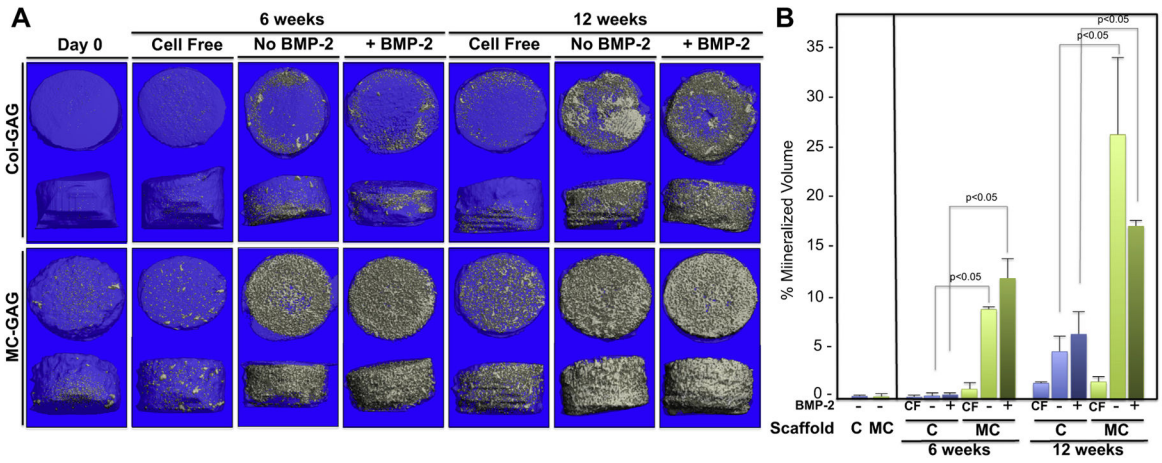

Fig. 4.

Mineralization on μCT scanning of hMSCs cultured on Col-GAG and MC-GAG scaffolds in the absence and presence of BMP-2. A) Representative 3D reconstructed μCT scans of histologic sections of collagen scaffolds cultured with hMSCs in osteogenic medium in the presence or absence of BMP-2 for 6 and 12 weeks on Col-GAG and MC-GAG scaffolds. B) Quantification of mineralized content on μCT scans in triplicate. CF, cell free.

Author Manuscript Author Manuscript Author Manuscript Author Manuscript

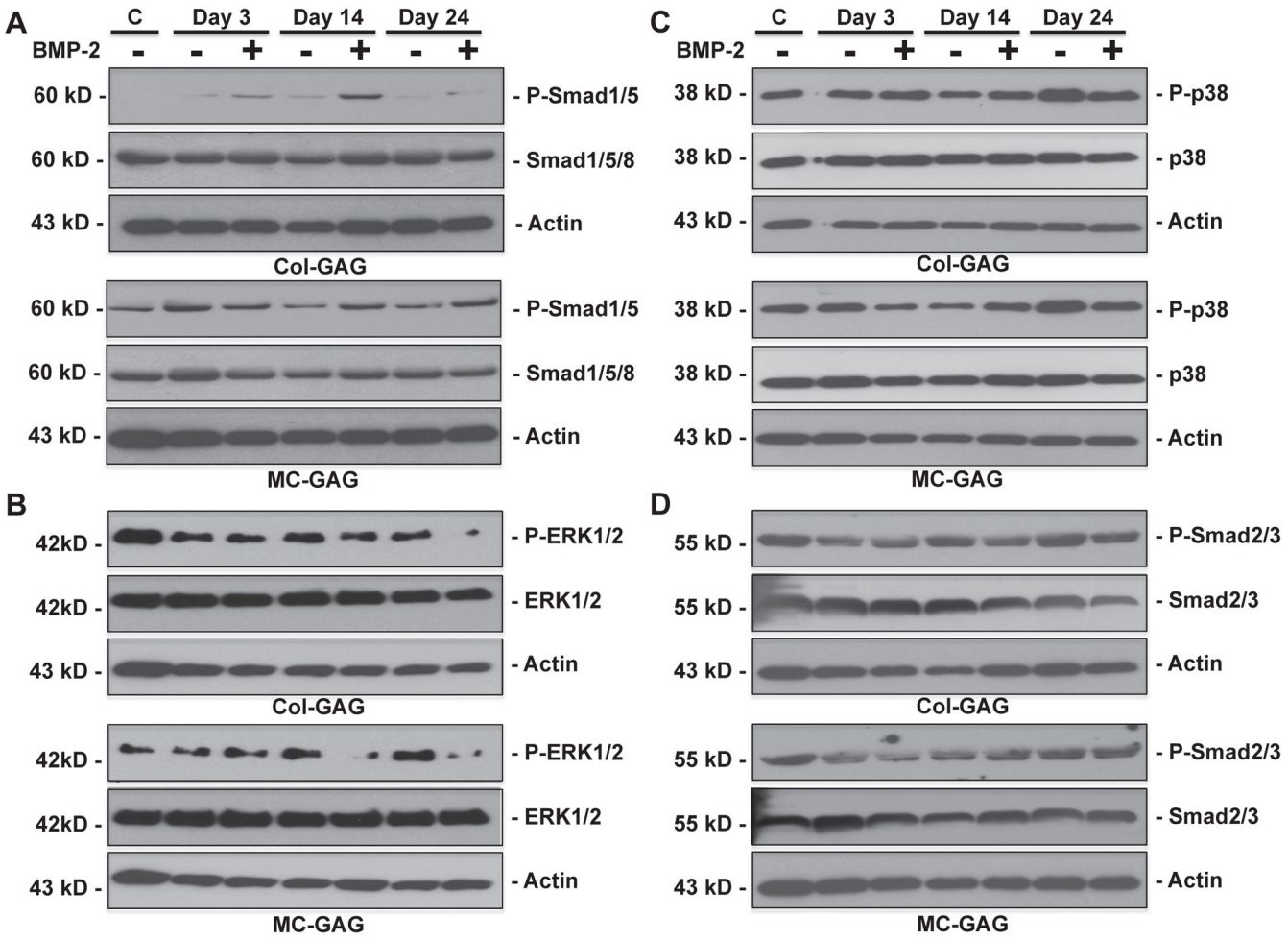

Fig. 5.

Elevated Smad1/5 phosphorylation and decreased ERK1/2 phosphorylation of hMSCs on MC-GAG scaffolds. Western blot of A) phosphorylated Smad1/5 (P-Smad1/5) and total Smad (Smad1/5/8), B) phosphorylated ERK1/2 (P-ERK1/2) and total ERK1/2, C) phosphorylated p38 (p-p38) and total p38, D) phosphorylated Smad2/3 and total Smad2/3. Actin controls are shown for each blot. All western blots were run in triplicate. A representative blot for each is shown.

Author Manuscript Author Manuscript Author Manuscript Author Manuscript

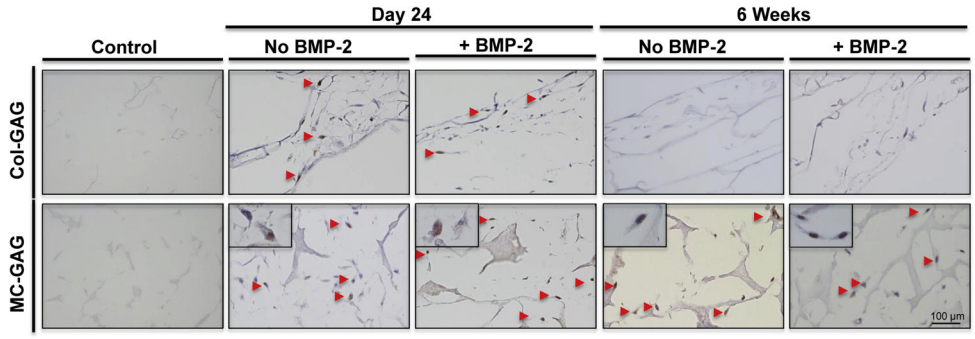

Fig. 6.

Phosphorylated Smad1/5 is localized in the nucleus of hMSCs on both Col-GAG and MC-GAG scaffolds. hMSCs cultured on Col-GAG and MC-GAG scaffolds were stained with anti-P-Smad1/5 at 24 days and 6 weeks in the absence and presence of BMP-2. Arrows denote nuclear staining. In the lower panels, high power inserts demonstrate nuclear staining.

Author Manuscript

Author Manuscript

Author Manuscript

Author Manuscript

Table 1

Primer sequences.

Genes	Oligonucleotide sequence
β-Actin sense	5′-TCACCCACACTGTGCCCCATCTACGA-3′
β-Actin antisense	5′-CAGCGGAACCGCTCATTGCCAATGG-3′
ALP sense	5′-TTGCGCACGTCATGGCCCTC-3′
ALP antisense	5′-CCCCATTAGGGGGCGTCACAT-3′
Col I sense	5′-TGCGACATGGACACTGGGGC-3′
Col I antisense	5′-GAGCCTTCGCTGCCGTACTCG-3′
OPN sense	5′-AGTCTGATGAGTCTGATGAAGTCAC-3′
OPN antisense	5′-GTGACTTTGGGTTTCCACGC-3′

ALP, alkaline phosphatase; Col I, type I collagen; OPN, Osteopontin.